

2017-09-15


Lipidomic Evaluation of Feline Neurologic Disease after AAV Gene Therapy

Heather L. Gray-Edwards
Auburn University

Et al.

Let us know how access to this document benefits you.

Follow this and additional works at: <https://escholarship.umassmed.edu/oapubs>

 Part of the [Animal Sciences Commons](#), [Congenital, Hereditary, and Neonatal Diseases and Abnormalities Commons](#), [Genetics and Genomics Commons](#), [Nervous System Diseases Commons](#), and the [Nutritional and Metabolic Diseases Commons](#)

Repository Citation

Gray-Edwards HL, Jiang X, Randle AN, Taylor AR, Voss TL, Johnson AK, McCurdy VJ, Sena-Esteves M, Ory DS, Martin DR. (2017). Lipidomic Evaluation of Feline Neurologic Disease after AAV Gene Therapy. Open Access Articles. <https://doi.org/10.1016/j.omtm.2017.07.005>. Retrieved from <https://escholarship.umassmed.edu/oapubs/3198>

Creative Commons License



This work is licensed under a [Creative Commons Attribution-Noncommercial-No Derivative Works 4.0 License](#). This material is brought to you by eScholarship@UMMS. It has been accepted for inclusion in Open Access Articles by an authorized administrator of eScholarship@UMMS. For more information, please contact Lisa.Palmer@umassmed.edu.

Lipidomic Evaluation of Feline Neurologic Disease after AAV Gene Therapy

Heather L. Gray-Edwards,¹ Xuntian Jiang,² Ashley N. Randle,¹ Amanda R. Taylor,³ Taylor L. Voss,¹ Aime K. Johnson,³ Victoria J. McCurdy,^{1,6} Miguel Sena-Esteves,⁴ Daniel S. Ory,² and Douglas R. Martin^{1,5}

¹Scott-Ritchey Research Center, Auburn University College of Veterinary Medicine, Auburn, AL 36849, USA; ²Diabetic Cardiovascular Disease Center, Washington University School of Medicine, St. Louis, MO 63130, USA; ³Department of Clinical Sciences, Auburn University College of Veterinary Medicine, Auburn, AL 36849, USA; ⁴Department of Neurology, University of Massachusetts Medical School, Worcester, PA 01655, USA; ⁵Department of Anatomy, Physiology, and Pharmacology, Auburn University, Auburn, AL 36849, USA

GM1 gangliosidosis is a fatal lysosomal disorder, for which there is no effective treatment. Adeno-associated virus (AAV) gene therapy in GM1 cats has resulted in a greater than 6-fold increase in lifespan, with many cats remaining alive at >5.7 years of age, with minimal clinical signs. Glycolipids are the principal storage product in GM1 gangliosidosis whose pathogenic mechanism is not completely understood. Targeted lipidomics analysis was performed to better define disease mechanisms and identify markers of disease progression for upcoming clinical trials in humans. 36 sphingolipids and subspecies associated with ganglioside biosynthesis were tested in the cerebrospinal fluid of untreated GM1 cats at a humane endpoint (~8 months), AAV-treated GM1 cats (~5 years old), and normal adult controls. In untreated GM1 cats, significant alterations were noted in 16 sphingolipid species, including gangliosides (GM1 and GM3), lactosylceramides, ceramides, sphingomyelins, monohexosylceramides, and sulfatides. Variable degrees of correction in many lipid metabolites reflected the efficacy of AAV gene therapy. Sphingolipid levels were highly predictive of neurologic disease progression, with 11 metabolites having a coefficient of determination (R^2) > 0.75. Also, a specific detergent additive significantly increased the recovery of certain lipid species in cerebrospinal fluid samples. This report demonstrates the methodology and utility of targeted lipidomics to examine the pathophysiology of lipid storage disorders.

INTRODUCTION

GM1 gangliosidosis is one of ~70 lysosomal storage disorders, with a prevalence of 1:7,700 live births.^{1,2} Deficiency of the enzyme β -galactosidase (EC 3.2.1.23) prevents degradation of GM1 ganglioside and its subsequent accumulation (or “storage”) within the lysosome. Lysosomal dysfunction ensues, resulting in a buildup of other molecules, many of which are complex lipids targeted for lysosomal degradation. Storage of these cellular materials ultimately results in fatal, neurologic disease that exists as four clinically distinct phenotypes based on the age at which symptoms appear: infantile, late infantile, juvenile, and adult onset.^{3,4}

A feline model of GM1 gangliosidosis was discovered in the 1970s and faithfully recapitulates human late-infantile/juvenile GM1 gangliosidosis.⁵ Since its discovery, feline GM1 gangliosidosis has been studied extensively and is an ideal large animal model to test novel therapeutics. We have developed an adeno-associated virus (AAV)-mediated gene therapy that results in extraordinary efficacy in GM1 animals, with greater than 6-fold extension in lifespan in the GM1 cat.^{6–10} Approximately half of the cats from the initial report⁹ are alive and healthy at a mean age of 6.4 ± 0.5 years. Even with such strong results, which have contributed to the planning of clinical trials, the pathogenic mechanism of lysosomal dysfunction in GM1 gangliosidosis remains incompletely defined, and there are few objective markers of disease progression appropriate for monitoring patients.

Tandem mass-spectrometry-based lipidomic analysis is a powerful technique with which to study pathways and networks of cellular lipids and to identify biomarkers of disease in glycolipidoses like GM1 gangliosidosis. In this study, we performed targeted lipidomics of cerebrospinal fluid (CSF) from cats with GM1 gangliosidosis, both untreated and ~5 years after AAV gene therapy. Our evaluation strategy consisted of lipids and subspecies (Figure 1) that were correlated with neurologic disease status to determine the predictive value of each analyte.

RESULTS

GM1 cats were treated with an intracranial injection of an AAVrh8 vector encoding feline β -galactosidase, as previously described.⁹ Approximately half of the cats from the original report are still healthy and have only mild neurological disease, as discussed in the companion manuscript (published in Molecular Therapy).¹⁰ The

Received 29 December 2016; accepted 22 July 2017;
<http://dx.doi.org/10.1016/j.omtm.2017.07.005>.

⁶Present address: Department of Biological Sciences, Mississippi State University, Starkville, MS 39762, USA.

Correspondence: Douglas R. Martin, Scott-Ritchey Research Center, Auburn University College of Veterinary Medicine and Department of Anatomy, Physiology, and Pharmacology, Auburn University, 1265 H.C. Morgan Drive, Auburn, AL 36849 USA.

E-mail: martidr@auburn.edu

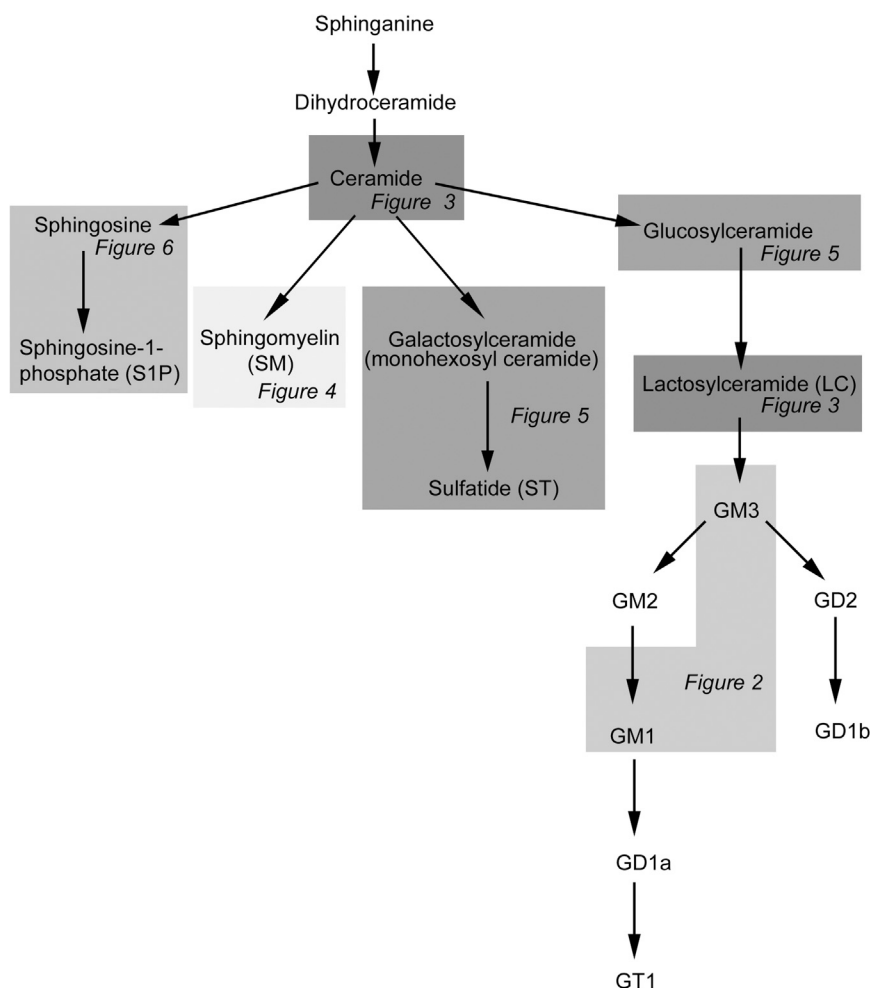


Figure 1. Glycosphingolipid Synthesis Pathway

Highlighted areas indicate metabolite alterations identified by targeted lipidomics in the CSF of cats with GM1 gangliosidosis, and associated figures in the current manuscript are shown.

therapy, most prominently for the 18:0 species (Figure 3D). Correlation with clinical signs was also strongest in the LC 18:0 species ($R^2 = 0.78$) compared to LC 16:0 ($R^2 = 0.43$) (Figures 3E and 3F). Although sphingomyelin (SM) is not in the same biosynthetic pathway as GM1 ganglioside, both molecules are assembled from a ceramide backbone. Five SM species (16:0, 18:0, 18:1, 20:0, and 22:0) were increased in the CSF of affected cats (Figures 4A, 4D, and 4G). SM alterations were reduced at variable levels in GM1 cats after AAV gene therapy (Figures 4A, 4D, and 4G). Correlation with the clinical rating score was strong ($R^2 > 0.80$) in SM 16:0, 18:0, 18:1, and 20:0 species (Figures 4B, 4C, 4E, and 4F).

Other lipids derived from ceramide were elevated in GM1 gangliosidosis. Sulfatides (STs) 18:0, 20:0, and 24:1 were elevated in GM1 cats, were completely or partially normalized after gene therapy, and correlated with clinical disease ($R^2 = 0.89$, $R^2 = 0.64$, and $R^2 = 0.51$, respectively) (Figure 5). Monohexosylceramide (MC) 16:0 and 18:0 were statistically increased in the CSF of GM1 cats, and levels of both MC 16:0 and MC 18:0 were partially normalized after gene therapy, which strongly correlated with clinical disease ($R^2 = 0.86$ and $R^2 = 0.75$, respectively).

main storage product in the brain of affected animals and humans, GM1 ganglioside isoforms (18:0 and 20:0) were markedly increased in the CSF of GM1 cats ($p < 0.01$). Approximately 5 years after gene therapy, GM1 remained at normal levels (Figure 2A). GM1 levels in CSF correlated strongly with clinical disease, with a coefficient of determination (R^2) of 0.92 and 0.97 for GM1 18:0 and 20:0, respectively (Figures 2B and 2C). Other components of the ganglioside biosynthetic pathway were altered as well. GM3 ganglioside (18:0 and 20:0) was elevated in untreated GM1 cats ($p < 0.01$), but remained at normal levels in AAV-treated animals (Figure 2D). Levels of GM3 18:0 and 20:0 correlated well with neurologic disease scores ($R^2 = 0.68$ and 0.72, respectively; Figures 2E and 2F).

Upstream in the ganglioside biosynthetic pathway (Figure 1), ceramide (Cer) and lactosylceramide (LC) were also altered in GM1 gangliosidosis. Cer (16:0 and 18:0) levels were increased in affected cats but remained normal in treated cats (Figure 3A). Clinical signs correlated with CSF concentrations of Cer 16:0 ($R^2 = 0.81$) and Cer 18:0 ($R^2 = 0.72$) (Figures 3B and 3C). LC (16:0 and 18:0) levels were also increased in GM1 cats, with normalization after gene

Other ceramide derivatives were measured in CSF, including sphingosine and sphingosine-1 phosphate (S1P), which were previously reported to be elevated in the CNS of mice with Sandhoff disease, a form of GM2 gangliosidosis.¹¹ Although sphingosine levels were 2-fold higher than normal in the CSF of affected cats and approached statistical significance ($p = 0.09$), S1P did not differ from normal (data not shown). Other lipids that were unchanged in treated and untreated GM1 cats included sphinganine, SM (24:0 and 26:0) and long chain MC species (20:0, 22:0, 24:0, and 24:1; data not shown).

The lack of significant amounts of proteins in CSF can result in the loss of lipophilic and highly protein-bound molecules through strong interactions with polypropylene container surfaces, such as hydrogen bonding, hydrophobic attractions, and ionic interactions. Detergents such as zwitterionic 3-[(3-cholamidopropyl) dimethylammonio]-1-propanesulfonate (CHAPS)¹² and Tween 80¹³ have been used as anti-adsorption agents for CSF sample analysis. Due to the

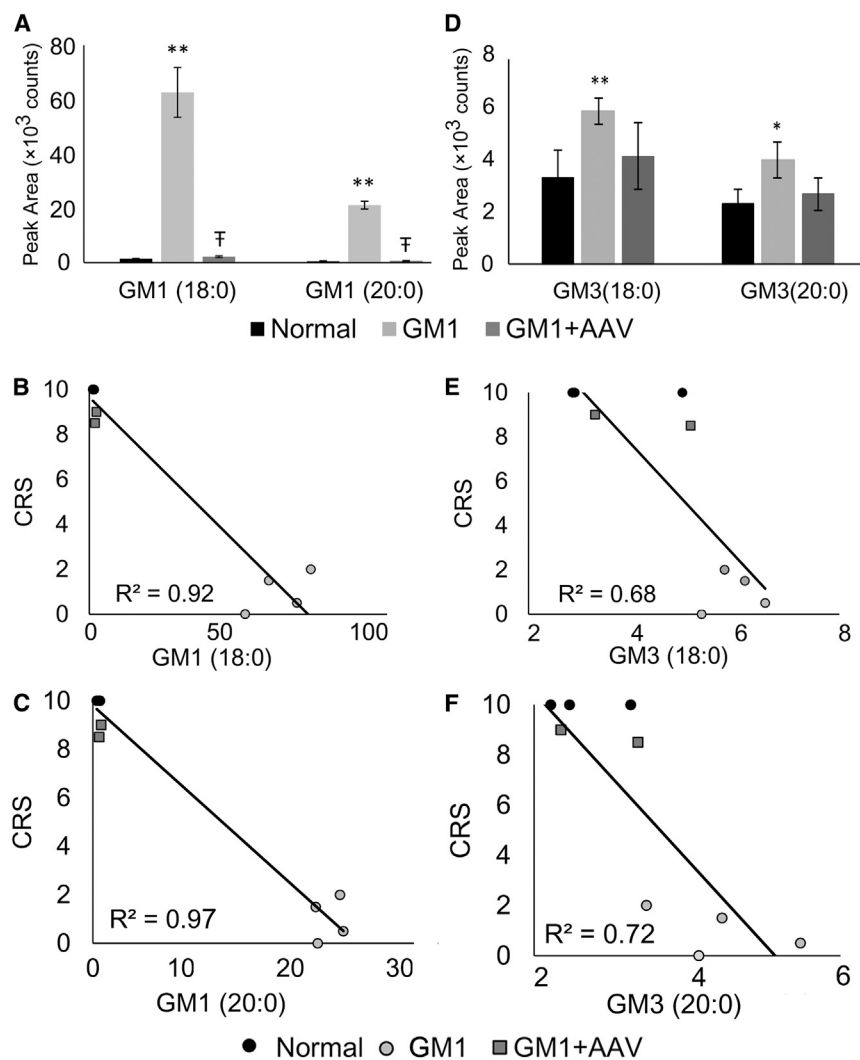


Figure 2. Lipidomic Alterations in the Ganglioside Biosynthetic Pathway

(A and D) Peak area (total counts) of gangliosides GM1 (A) and GM3 (D) in normal cats, untreated GM1 cats, and GM1 cats ~5 years after gene therapy (GM1+AAV). All samples were run in the same batch. * $p < 0.05$ from normal; ** $p < 0.01$ from normal; ‡ $p < 0.05$ from untreated GM1; † $p < 0.01$ from untreated GM1. (B, C, E, F) Correlation of ganglioside levels in CSF with clinical rating score (CRS) of normal, GM1, and GM1+AAV cats. The precise ganglioside species is noted below each scatterplot, and R^2 is shown on the scatterplots. Normal cats, $n = 4$; GM1, $n = 4$; GM1+AAV, $n = 2$. Error bars represent SD.

available for clinical trial recruitment, and clinicians must rely on predictive outcome measures to determine therapeutic efficacy. Also, although β -galactosidase deficiency is the proximate cause of disease, further elucidation of the precise pathogenic mechanism is needed. For these reasons, we evaluated MRI, CSF, blood, and electrodiagnostic biomarkers in cats and humans with GM1 gangliosidosis (please refer to the companion manuscript published in Molecular Therapy¹⁰). For a more thorough analysis of the precise lipid abnormalities in GM1 gangliosidosis, here we performed targeted lipidomic analysis of CSF from untreated and AAV-treated GM1 cats. We used LC-tandem mass spectrometry (LC-MS/MS)-based lipidomic profiling to identify sphingolipid metabolites altered in feline GM1 gangliosidosis that respond to AAV gene therapy and reflected the clinical status of the animal. Because many of the lipid alterations in GM1 gangliosidosis correlate strongly

with neurologic disease, they may be useful objective measures to assess disease status in clinical trials.

hydrophobic nature of lipid metabolites and their electrostatic interactions with many plastics, CSF for this study was collected into tubes pre-coated with CHAPS (see Materials and Methods for more information). Because the addition of the detergent to CSF collection tubes is not routine and banked, non-detergent-containing CSF samples from GM1 cats and humans are extensive, we performed a direct comparison of CSF samples in the presence or absence of detergent. Significant loss of sphingosine, GM3 22:0, SM 22:0, and SM 24:0 was noted without detergent (Figure 6). Also, losses of SM 18:1 and SM 20:0 from CSF without detergent trended toward significance ($p = 0.056$ and 0.054 , respectively). GM1 ganglioside (18:0 or 20:0) concentration was not significantly reduced in the absence of the detergent additive.

DISCUSSION

Currently, there is no effective treatment for GM1 gangliosidosis. As a rare disorder, GM1 gangliosidosis has a small number of patients

GM1 gangliosidosis is named for its primary storage product, GM1 ganglioside, which was virtually cleared from the brain of affected mice and cats after AAV gene therapy.^{8,9} Because many treated cats are still alive and healthy at >5 years post-treatment, we decided to analyze CSF for GM1 ganglioside levels as both an indicator of neurologic disease in the cats and a clinically useful metric for human patients. GM1 levels in CSF strongly correlated with clinical disease and, in AAV-treated GM1 cats, were completely normal (i.e., ~3% of the level in untreated cats for both the 18:0 and 20:0 species; Figure 2). Of the 36 lipid species analyzed in this study, GM1 ganglioside was the most reliable and robust indicator of disease progression, as expected.

Gangliosides are amphiphilic, with a ceramide core and a polysaccharide side chain with or without sialic acid. The earliest and least

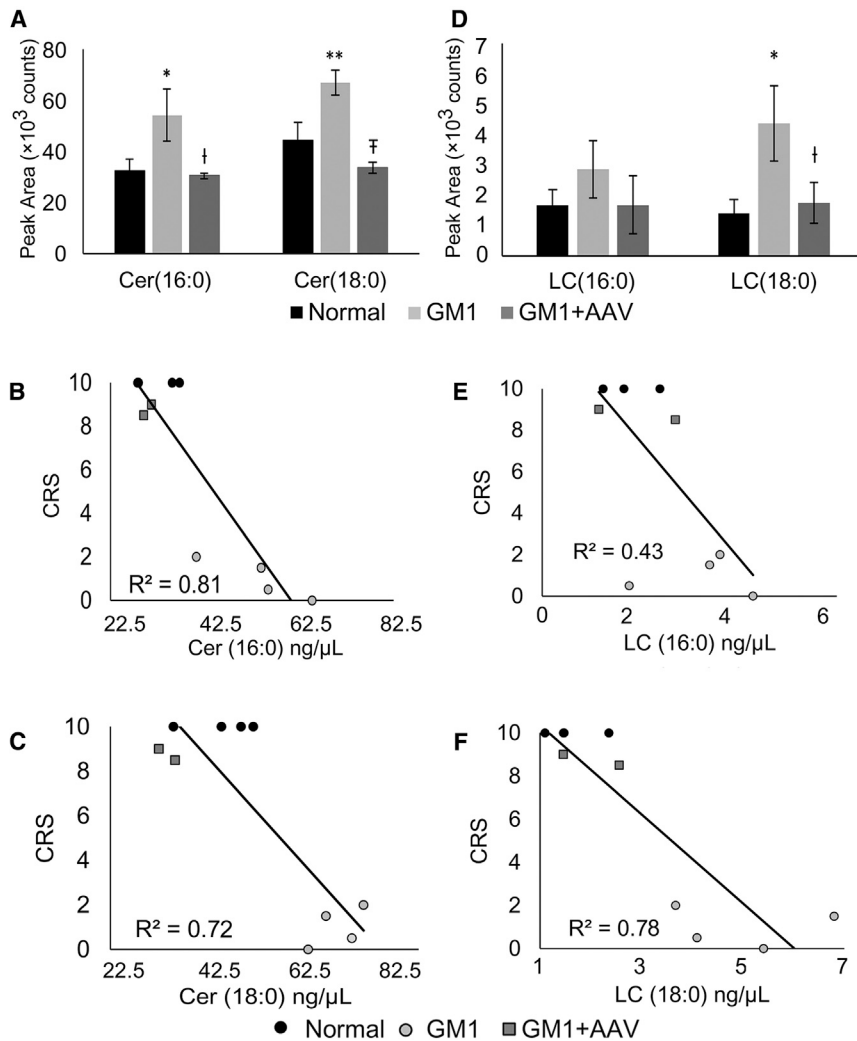


Figure 3. Cer and LC Alterations in GM1 Gangliosidosis Cats

(A and D) Peak area (total counts) of Cer 16:0 and 18:0 (A) and LC 16:0 and 18:0 (D). All samples were run in the same batch. * $p < 0.05$ from normal; ** $p < 0.01$ from normal; † $p < 0.05$ from GM1; ‡ $p < 0.01$ from GM1. (B, C, E, and F) Correlation of CRS of normal, GM1, and GM1+AAV cats with metabolite levels for Cer (B and C) and LC (E and F) species. R^2 values are denoted on the graphs. Normal cats, $n = 4$; GM1, $n = 4$; GM1+AAV, $n = 2$. Error bars represent SD.

cats with GM1 gangliosidosis (Figures 3 and 5), inversely correlating with reduced levels in the brains of GM1 mice, as previously reported.^{6,8} Although the results are potentially contradictory, we hypothesize a mechanism for cellular release of complex lipids from the brain into CSF during myelin loss. Similarly, SM elevations in the CSF of GM1 cats may also be explained by shedding into CSF as myelin deteriorates. With gene therapy, CSF from GM1 cats showed a strong pattern of normalization for SM, ST, and cerebrosides. These data support MRI and magnetic resonance (MR) spectroscopy results, which show that AAV gene therapy preserves or restores myelination in the GM1 cat.^{9,10}

The use of CSF sphingolipids to evaluate disease progression in lysosomal storage diseases was first proposed in 1992.²¹ Since then, MS-based metabolomic markers have been developed for animal models of Krabbe disease,^{22,23} multiple sclerosis,^{24,25} Alzheimer disease,^{26,27} hydrocephalus,²⁸ Parkinson disease,²⁹ amyotrophic

lateral sclerosis,³⁰ and glioma.³¹ MS-based lipidomics in Niemann-Pick disease previously showed high sensitivity and specificity in detecting treatment responses in the plasma and brain.³² Future studies will determine if the invasiveness of CSF collection is required to accurately track therapeutic efficacy in GM1 gangliosidosis or whether peripheral blood samples will suffice.

In conclusion, targeted lipidomic profiling has identified several lipid molecules and subspecies that correlate strongly with disease status and reflect efficacy of gene therapy in feline GM1 gangliosidosis. The array of markers identified herein may facilitate a more thorough understanding of disease mechanism and provide objective outcome measures for future clinical trials.

MATERIALS AND METHODS

CSF Collection

All animal procedures were approved by the Institutional Animal Care and Use Committee at Auburn University. GM1 cats were treated by

complex ganglioside, GM3 is present in the CNS but is more abundant in the periphery. It functions in cell proliferation, differentiation, embryogenesis, apoptosis, oncogenesis, and insulin resistance.^{14,15} Secondary increases of GM3 have been reported in several lysosomal storage disorders, including the mucopolysaccharidoses,¹⁶ Niemann-Pick disease type C,¹⁷ Gaucher disease,^{18,19} and GM2 gangliosidosis,²⁰ where its accumulation is thought to result from generalized lysosomal dysfunction rather than a primary enzyme deficiency. As in other lysosomal disorders, GM3 was elevated significantly in cats with GM1 gangliosidosis, at least in CSF (Figure 2). Its return to normal levels after gene therapy probably represents restored function of the lysosomal trafficking and/or degradative system.

Demyelination is a prominent feature of gangliosidosis and is thought to correlate with MRI signal intensity changes of white matter as neurodegeneration progresses. Several of the lipid species analyzed herein are components of myelin, including SM, sulfatides, and cerebrosides (LC and MC). Sulfatides and cerebrosides were elevated in the CSF of

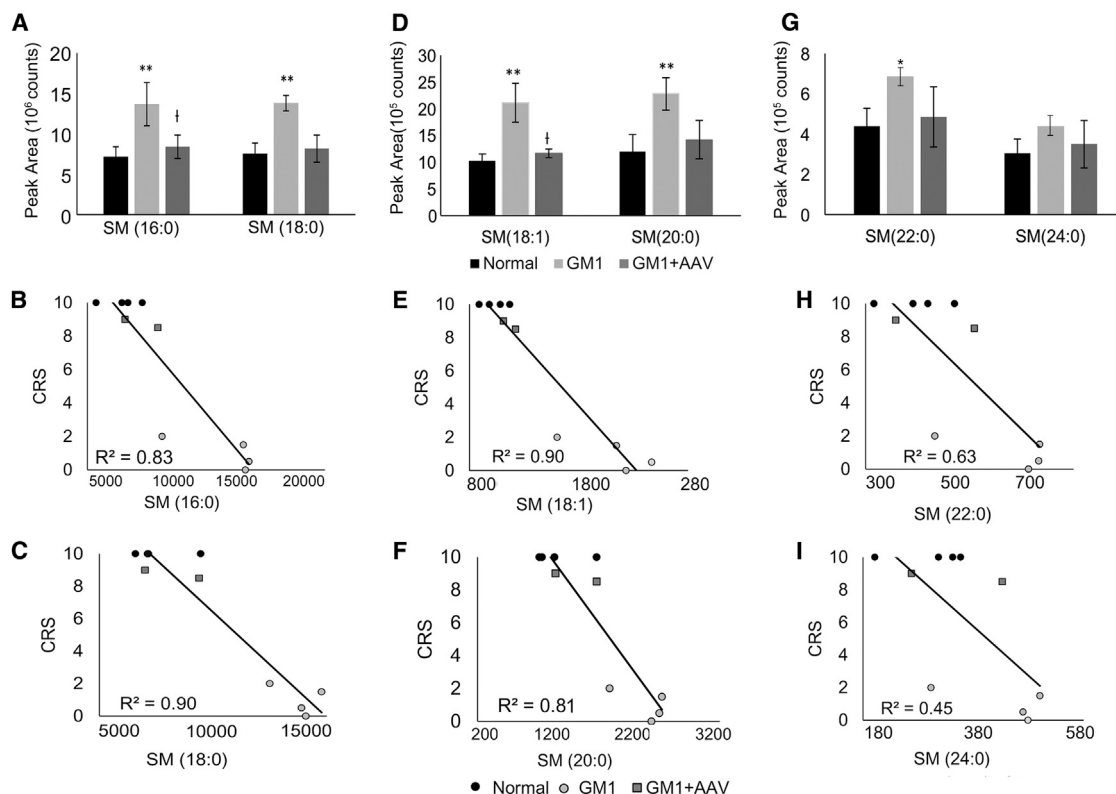


Figure 4. SM in CSF of Cats

(A, D, and G) SM species levels increase in untreated GM1 cats. After gene therapy, SM species returned to normal. All samples were run in the same batch. * $p < 0.05$ from normal; ** $p < 0.01$ from normal; † $p < 0.05$ from GM1; ‡ $p < 0.01$ from GM1. (B, C, E, F, H, and I) Correlation of SM levels with the CRS of normal, GM1, and GM1+AAV cats. R^2 values are denoted on the graphs. Normal cats, $n = 4$; GM1, $n = 4$; GM1+AAV, $n = 2$. Error bars represent SD.

bilateral injections of the thalamus and deep cerebellar nuclei using an AAVrh8 vector encoding feline β -galactosidase, as previously described.⁹ Cats were treated at 1.3 to 3 months of age, prior to symptom onset. Clinical rating scores were determined based on clinical signs with a normal score of ten and subtraction of one point for each symptom acquired: slight tremors, overt tremors, paraparesis, wide-based stance, ataxia, occasional falling, limited ambulation, spastic thoracic limbs, spastic pelvic limbs, and inability to ambulate.

For CSF collection, normal ($n = 4$), GM1 ($n = 4$), and AAV-treated GM1 cats ($n = 2$) were anesthetized using a combination of dexmedetomidine and ketamine, intubated, and maintained at an appropriate anesthetic plane using isoflurane. The skin was clipped and aseptically prepared above the cisterna magna, from which CSF was collected with a spinal needle. CSF was allowed to drop into empty polypropylene tubes and polypropylene tubes pre-coated with CHAPS at a ratio of 20 μ L of 0.5 g/mL w/v CHAPS per 500 μ L of CSF. CSF samples were stored at -80°C until analysis.

LC-MS/MS Lipidomics

LC-MS/MS analysis was conducted on a Shimadzu Prominence UFLC system coupled with an Applied Biosystems/MDS Sciex

4000QTRAP mass spectrometer using multiple reaction monitoring (MRM) and two Valco switching valves. The CSF samples were injected directly to the LC-MS/MS system. A quality control sample was prepared by pooling 20 μ L from each study sample, and injected every three study samples to monitor the instrument performance. The relative quantification data were measured as peak areas of analytes and reported as total counts. All the samples were analyzed in one batch so that relative comparisons could be made accurately without run-to-run variation. The coefficient of variation of each lipid in the quality control sample was less than 15%, indicating that the mass spectrometric response was reproducible within the batch.

LC-MS/MS Analysis of Cer, MC, LC, and SM

Separation of Cer, MC, LC, and SM was carried out at 50°C using a Waters XBridge C18 analytical column (3×100 mm, $3 \mu\text{m}$) connected to a Phenomenex SecurityGuard C18 guard column (4×3 mm) at a flow rate of 0.4 mL/min. The mobile phase consisted of 20 mM ammonium acetate in water (solvent A) and tetrahydrofuran-methanol (6:94) (solvent B). The step gradient was as follows: 0–5 min, 95%–100% solvent B; 5–8.5 min, 100% solvent B; 8.5–8.6 min, 100%–95% solvent B; and 8.6–13 min, 95% solvent B. The effluent was directed into the mass spectrometer for data

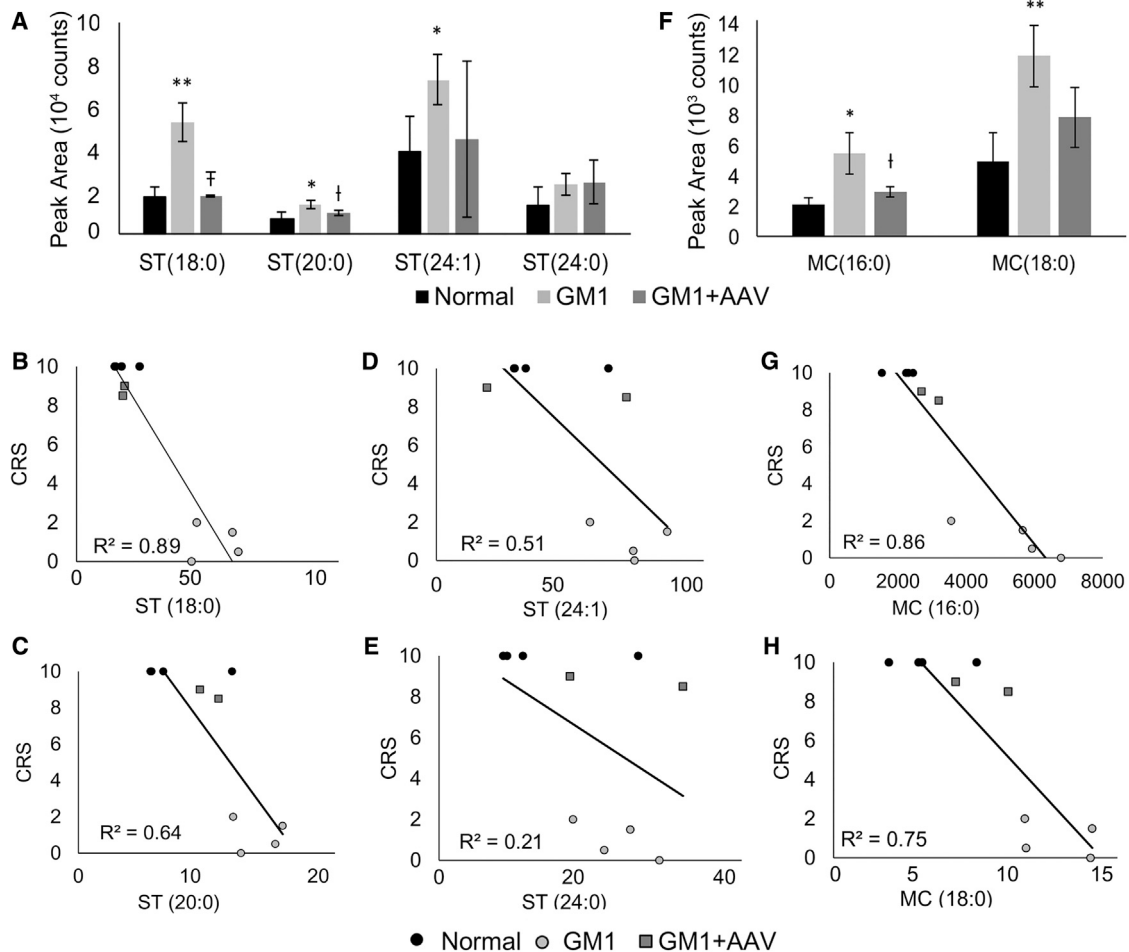


Figure 5. ST and MC in CSF of GM1 Cats

(A and F) Peak areas (total counts) of ST (A) and MC (F) in CSF. All samples were run in the same batch. * $p < 0.05$ from normal; ** $p < 0.01$ from normal; † $p < 0.05$ from GM1; ‡ $p < 0.01$ from GM1. (B–E, G, and H) Correlation of ST (B–E) and MC (G and H) with clinical disease in normal, GM1, and GM1+AAV cats. R^2 values are denoted on the graphs. Normal cats, $n = 4$; GM1, $n = 4$; GM1+AAV, $n = 2$. Error bars represent SD.

acquisition within the 6-min time window (3–9 min); elsewhere, effluent was sent to waste to minimize source contamination. The column was back flushed with isopropanol at 1 mL/min from 8.5 to 10.5 min. The injection volume was 10 μ L, and the total run time was 13 min. The electrospray ionization (ESI) source temperature was 550°C; the ESI needle was 5,000 V. The collision and curtain gas were set at medium and 20, respectively. Both desolvation gas and nebulizing gas were set at 35 L/min. The MRM transitions for Cer(16:0), Cer(18:0), MC(16:0), MC(18:0), MC(20:0), MC(22:0), MC(24:0), MC(24:1), LC(16:0), LC(18:0), SM(16:0), SM(18:0), SM(18:1), SM(20:0), SM(22:0), SM(24:0), and SM(24:1) were from 538.5 to 264.3, 566.5 to 264.3, 700.5 to 264.3, 728.5 to 264.3, 756.5 to 264.3, 784.5 to 264.3, 812.5 to 264.3, 810.5 to 264.3, 862.7 to 264.3, 890.7 to 264.3, 703.5 to 184, 731.5 to 184, 729.5 to 184, 759.5 to 184, 787.5 to 184, 815.7 to 184, and 813.7 to 184, respectively. The declustering potential (DP), entrance potential (EP), collision energy (CE), and collision cell exit potential (CXP) for Cer were 70 V,

10 V, 35 V, and 6 V, respectively. The DP, EP, CE, and CXP for MC were 75 V, 10 V, 50 V, and 6 V, respectively. The DP, EP, CE, and CXP for LC were 80 V, 10 V, 61 V, and 10 V, respectively. The DP, EP, CE, and CXP for SM were 100 V, 10 V, 40 V, and 10 V, respectively. The dwell time was set at 20 ms for each MRM transition. Data were acquired and analyzed by Analyst software (version 1.5.2).

LC-MS/MS Analysis of GM1, GM3, and ST

Separation of GM1, GM3, and ST was carried out at room temperature using an Advanced Chromatography Technologies ACE Super C18 analytical column (3 \times 100 mm, 3 μ m) connected to a Phenomenex SecurityGuard Gemini C18 guard column (4 \times 3 mm) at a flow rate of 1 mL/min. The mobile phase consisted of 2.9 mM diethylamine and 20 mM hexafluoro-2-propanol in water (solvent A) and methanol-tetrahydrofuran (97:3) (solvent B). The step gradient was as follows: 0–4 min, 90%–100% solvent B; 4–5 min, 100% solvent B; 5–5.1 min, 100%–90% solvent B; and 5.1–8.5 min, 90%

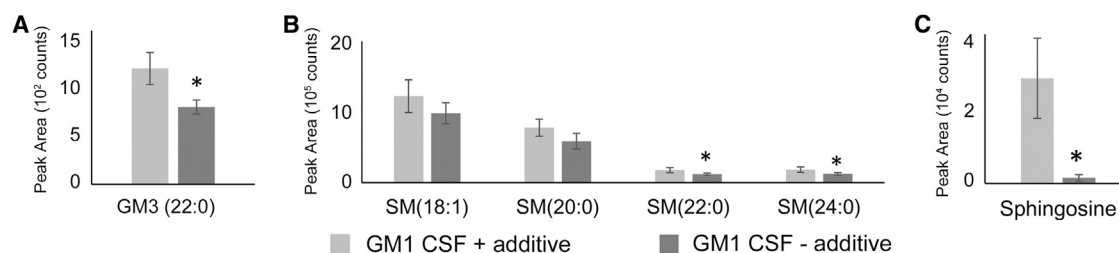


Figure 6. Comparison of Metabolite Levels in CSF Collected with or without Detergent Additive

Samples were collected from untreated GM1 cats and subdivided into two tubes: one with detergent and one without. (A–C) Levels of GM3 (22:0) (A) SM (22:0) (B), SM (24:0) (B), and sphingosine (C) were reduced in the absence of detergent. SM 18:1 and 20:0 reductions did not reach statistical significance ($p = 0.056$ and 0.054 , respectively). * $p < 0.05$ from CSF with additive. Error bars represent SD.

solvent B. The effluent was directed into the mass spectrometer for data acquisition within the 3.5-min time window (1.5–5 min); elsewhere, effluent was sent to waste to minimize source contamination. The column was back flushed with isopropanol at 1 mL/min from 4.5 to 6 min. The injection volume was 10 μ L, and the total run time was 8.5 min. The ESI source temperature was 500°C; the ESI needle was –4,500 V. The collision and curtain gas were set at medium and 20, respectively. The desolvation gas and nebulizing gas were set at 35 and 55 L/min, respectively. The MRM transitions for GM1(18:0), GM1(20:0), GM3(18:0), GM3(20:0), ST(18:0), ST(20:0), ST(22:0), ST(24:1), and ST(24:0) were from 1,544.9 to 290.2, 1,572.9 to 290.2, 1,179.9 to 290.2, 1,207.9 to 290.2, 806.6 to 97, 834.6 to 97, 862.6 to 97, 888.6 to 97, and 890.6 to 97, respectively. The DP, EP, CE, and CXP for GM1 were –210 V, –10 V, –97 V, and –4 V, respectively. The DP, EP, CE, and CXP for GM3 were –220 V, –10 V, –68 V, and –4 V, respectively. The DP, EP, CE, and CXP for ST were –200 V, –10 V, –129 V, and –6 V, respectively. The dwell time was set at 20 ms for each of MRM transition. Data were acquired and analyzed by Analyst software (version 1.5.2).

LC-MS/MS Analysis of Sphingosine and Sphinganine

Separation of sphingosine and sphinganine was carried out at room temperature using a Waters XBridge C8 analytical column (3 \times 50 mm, 3.5 μ m) connected to a Phenomenex SecurityGuard C18 guard column (4 \times 3 mm) at a flow rate of 0.6 mL/min. The mobile phase consisted of 0.1% formic acid in water (solvent A) and 0.1% formic acid in methanol-acetonitrile (4:1) (solvent B). The step gradient was as follows: 0–3 min, 70%–100% solvent B; 3–3.5 min, 100% solvent B; 3.5–3.6 min, 100%–70% solvent B; and 3.6–8 min, 70% solvent B. The effluent was directed into the mass spectrometer for data acquisition within the 3.5-min time window (1.5–3.5 min); elsewhere, effluent was sent to waste to minimize source contamination. The column was back flushed with isopropanol at 0.6 mL/min from 3.5 to 6.5 min. The injection volume was 10 μ L, and the total run time was 8 min. The ESI source temperature was 550°C; the ESI needle was 5,000 V. The collision and curtain gas were set at medium and 20, respectively. Both desolvation gas and nebulizing gas were set at 35 L/min. The dwell time was set at 20 ms for each MRM transition. The MRM transitions for sphingosine and sphinganine were from 300.4 to 252.3 and 302.4 to 254.3, respectively. The

DP, EP, CE, and CXP for sphingosine were 50 V, 10 V, 24 V, and 6 V, respectively. The DP, EP, CE, and CXP for sphinganine were 80 V, 10 V, 30 V, and 10 V, respectively. Data were acquired and analyzed by Analyst software (version 1.5.2).

Statistics

Statistical analyses were performed using a two-tailed, paired Student's *t* test, assuming unequal variances. *p* values of < 0.05 and < 0.01 are compared to normal (* and **, respectively) and untreated GM1 cats (\dagger and \ddagger , respectively). Error bars represent SD.

Study Approval

All animal studies were performed in accordance with the Auburn University Institutional Animal Care and Use Committee.

AUTHOR CONTRIBUTIONS

H.L.G.-E. was the primary author on the manuscript, collected CSF, and performed the majority of cat data analyses and interpretation. X.J. was responsible for lipidomics data acquisition and participated in study design and data interpretation. A.N.R. and A.K.J. performed cat surgeries and anesthesia and contributed to manuscript preparation. T.L.V. performed regression analyses and other data analysis and assisted with authorship. A.R.T. contributed to data interpretation and manuscript preparation and also collected CSF. V.J.M. assisted in study design, biomarker development, and evaluation of therapeutic benefit. M.S.-E. designed and produced the AAV vectors for this project and participated in study design. D.S.O. designed the lipidomics analysis, was responsible for data interpretation, and contributed to manuscript preparation. D.R.M. was responsible for overall study design and data interpretation, managed all research studies described herein, and assisted in authorship.

CONFLICTS OF INTEREST

D.R.M. and M.S.-E. are shareholders in Lysogene (Neuilly-sur-Seine, France).

ACKNOWLEDGMENTS

These studies were funded in part by NIH grants R01 HD060576 (D.R.M. and M.S.-E.), R01 NS081985 (D.S.O.), and F32 NS080488 (H.L.G.-E.) and NIH CTSA grant UL1 TR000448 (X.J.).

REFERENCES

- Meikle, P.J., Hopwood, J.J., Clague, A.E., and Carey, W.F. (1999). Prevalence of lysosomal storage disorders. *JAMA* 281, 249–254.
- Cox, T.M., and Cachón-González, M.B. (2012). The cellular pathology of lysosomal diseases. *J. Pathol.* 226, 241–254.
- Regier, D.S., and Tiffit, C.J. (2013). GLB1-related disorders. In *GeneReviews*(R), R.A. Pagon, M.P. Adam, H.H. Ardinger, S.E. Wallace, A. Amemiya, L.J.H. Bean, T.D. Bird, N. Ledbetter, H.C. Mefford, and R.J.H. Smith, et al., eds. (University of Washington).
- Suzuki, Y., Hitoshi, S., and Oshima, A. (1995). Beta-galactosidase deficiency(beta-galactosidosis): GM1 gangliosidosis and Morquio disease. In *The Metabolic and Molecular Bases of Inherited Diseases, Volume II*, C.R. Scriver, A.L. Beaudet, W.S. Sly, and D. Valle, eds. (McGraw-Hill).
- Baker, H.J., Jr., Lindsey, J.R., McKhann, G.M., and Farrell, D.F. (1971). Neuronal GM1 gangliosidosis in a Siamese cat with beta-galactosidase deficiency. *Science* 174, 838–839.
- Broekman, M.L., Baek, R.C., Comer, L.A., Fernandez, J.L., Seyfried, T.N., and Sena-Esteves, M. (2007). Complete correction of enzymatic deficiency and neurochemistry in the GM1-gangliosidosis mouse brain by neonatal adeno-associated virus-mediated gene delivery. *Mol. Ther.* 15, 30–37.
- Weismann, C.M., Ferreira, J., Keeler, A.M., Su, Q., Qui, L., Shaffer, S.A., Xu, Z., Gao, G., and Sena-Esteves, M. (2015). Systemic AAV9 gene transfer in adult GM1 gangliosidosis mice reduces lysosomal storage in CNS and extends lifespan. *Hum. Mol. Genet.* 24, 4353–4364.
- Baek, R.C., Broekman, M.L., Leroy, S.G., Tierney, L.A., Sandberg, M.A., d'Azzo, A., Seyfried, T.N., and Sena-Esteves, M. (2010). AAV-mediated gene delivery in adult GM1-gangliosidosis mice corrects lysosomal storage in CNS and improves survival. *PLoS ONE* 5, e13468.
- McCurdy, V.J., Johnson, A.K., Gray-Edwards, H.L., Randle, A.N., Brunson, B.L., Morrison, N.E., Salibi, N., Johnson, J.A., Hwang, M., Beyers, R.J., et al. (2014). Sustained normalization of neurological disease after intracranial gene therapy in a feline model. *Sci. Transl. Med.* 6, 231ra48.
- Gray-Edwards, H.L., Regier, D.S., Shirley, J.L., Randle, A.N., Salibi, N., Thomas, S.E., Latour, Y.L., Johnston, J., Golas, G., Maguire, A.S., et al. (2017). Novel biomarkers of human GM1 gangliosidosis reflect the clinical efficacy of gene therapy in a feline model. *Mol. Ther.* 25, 892–903.
- Wu, Y.P., Mizugishi, K., Bektas, M., Sandhoff, R., and Proia, R.L. (2008). Sphingosine kinase 1/S1P receptor signaling axis controls glial proliferation in mice with Sandhoff disease. *Hum. Mol. Genet.* 17, 2257–2264.
- Kadar, E.P., Su, Y., Zhang, Y., Tweed, J., and Wujcik, C.E. (2010). Evaluation of the relationship between a pharmaceutical compound's distribution coefficient, log D and adsorption loss to polypropylene in urine and CSF. *Bioanalysis* 2, 755–767.
- Gu, H., Deng, Y., Wang, J., Aubry, A.F., and Arnold, M.E. (2010). Development and validation of sensitive and selective LC-MS/MS methods for the determination of BMS-708163, a gamma-secretase inhibitor, in plasma and cerebrospinal fluid using deprotonated or formate adduct ions as precursor ions. *J. Chromatogr. B Analyt. Technol. Biomed. Life Sci.* 878, 2319–2326.
- Prokazova, N.V., Samoilova, N.N., Gracheva, E.V., and Golovanova, N.K. (2009). Ganglioside GM3 and its biological functions. *Biochemistry (Mosc.)* 74, 235–249.
- Tagami, S., Inokuchi Ji, J., Kabayama, K., Yoshimura, H., Kitamura, F., Uemura, S., Ogawa, C., Ishii, A., Saito, M., Ohtsuka, Y., et al. (2002). Ganglioside GM3 participates in the pathological conditions of insulin resistance. *J. Biol. Chem.* 277, 3085–3092.
- Ohmi, K., Greenberg, D.S., Rajavel, K.S., Ryazantsev, S., Li, H.H., and Neufeld, E.F. (2003). Activated microglia in cortex of mouse models of mucopolysaccharidoses I and IIIB. *Proc. Natl. Acad. Sci. USA* 100, 1902–1907.
- Vanier, M.T. (2015). Complex lipid trafficking in Niemann-Pick disease type C. *J. Inher. Metab. Dis.* 38, 187–199.
- Nilsson, O., Månsson, J.E., Håkansson, G., and Svennerholm, L. (1982). The occurrence of psychosine and other glycolipids in spleen and liver from the three major types of Gaucher's disease. *Biochim. Biophys. Acta* 712, 453–463.
- Nilsson, O., and Svennerholm, L. (1982). Accumulation of glucosylceramide and glucosylsphingosine (psychosine) in cerebrum and cerebellum in infantile and juvenile Gaucher disease. *J. Neurochem.* 39, 709–718.
- Gravel, R.A., Clarke, J.T., Kaback, M.M., Mahuran, D., Sandhoff, K., and Suzuki, K. (1995). The GM2 gangliosidoses. In *The Metabolic and Molecular Bases of Inherited Disease, Seventh Edition, Volume II*, C.R. Scriver, A.L. Beaudet, W.S. Sly, and D. Valle, eds. (McGraw-Hill).
- Kaye, E.M., Ullman, M.D., Kolodny, E.H., Krivit, W., and Rischert, J.C. (1992). Possible use of CSF glycosphingolipids for the diagnosis and therapeutic monitoring of lysosomal storage diseases. *Neurology* 42, 2290–2294.
- Esch, S.W., Williams, T.D., Biswas, S., Chakrabarty, A., and LeVine, S.M. (2003). Sphingolipid profile in the CNS of the twitcher (globoid cell leukodystrophy) mouse: a lipidomics approach. *Cell. Mol. Biol.* 49, 779–787.
- Bradbury, A.M., Bagel, J.H., Jiang, X., Swain, G.P., Prociuk, M.L., Fitzgerald, C.A., O'Donnell, P.A., Braund, K.G., Ory, D.S., and Vite, C.H. (2016). Clinical, electrophysiological, and biochemical markers of peripheral and central nervous system disease in canine globoid cell leukodystrophy (Krabbe's disease). *J. Neurosci. Res.* 94, 1007–1017.
- Gonzalo, H., Brieva, L., Tatzber, F., Jové, M., Cacabelos, D., Cassanyé, A., Lanau-Angulo, L., Boada, J., Serrano, J.C., González, C., et al. (2012). Lipidome analysis in multiple sclerosis reveals protein lipoxidative damage as a potential pathogenic mechanism. *J. Neurochem.* 123, 622–634.
- Vidaurre, O.G., Haines, J.D., Katz Sand, I., Adula, K.P., Huynh, J.L., McGraw, C.A., Zhang, F., Varghese, M., Sotirchos, E., Bhargava, P., et al. (2014). Cerebrospinal fluid ceramides from patients with multiple sclerosis impair neuronal bioenergetics. *Brain* 137, 2271–2286.
- Koal, T., Klavins, K., Seppi, D., Kemmler, G., and Humpel, C. (2015). Sphingomyelin SM(d18:1/18:0) is significantly enhanced in cerebrospinal fluid samples dichotomized by pathological amyloid-β42, tau, and phospho-tau-181 levels. *J. Alzheimers Dis.* 44, 1193–1201.
- Trushina, E., Dutta, T., Persson, X.M., Mielke, M.M., and Petersen, R.C. (2013). Identification of altered metabolic pathways in plasma and CSF in mild cognitive impairment and Alzheimer's disease using metabolomics. *PLoS ONE* 8, e63644.
- Huang, H., Yang, J., Luciano, M., and Shriver, L.P. (2016). Longitudinal metabolite profiling of cerebrospinal fluid in normal pressure hydrocephalus links brain metabolism with exercise-induced VEGF production and clinical outcome. *Neurochem. Res.* 41, 1713–1722.
- Trupp, M., Jonsson, P., Ohrfelt, A., Zetterberg, H., Obudulu, O., Malm, L., Wuolikainen, A., Linder, J., Moritz, T., Blennow, K., et al. (2014). Metabolite and peptide levels in plasma and CSF differentiating healthy controls from patients with newly diagnosed Parkinson's disease. *J. Parkinsons Dis.* 4, 549–560.
- Blasco, H., Corcia, P., Pradat, P.F., Bocca, C., Gordon, P.H., Veyrat-Durebex, C., Mavel, S., Nadal-Desbarats, L., Moreau, C., Devos, D., et al. (2013). Metabolomics in cerebrospinal fluid of patients with amyotrophic lateral sclerosis: an untargeted approach via high-resolution mass spectrometry. *J. Proteome Res.* 12, 3746–3754.
- Nakamizo, S., Sasayama, T., Shinohara, M., Irino, Y., Nishiumi, S., Nishihara, M., Tanaka, H., Tanaka, K., Mizukawa, K., Itoh, T., et al. (2013). GC/MS-based metabolomic analysis of cerebrospinal fluid (CSF) from glioma patients. *J. Neurooncol.* 113, 65–74.
- Fan, M., Sidhu, R., Fujiwara, H., Tortelli, B., Zhang, J., Davidson, C., Walkley, S.U., Bagel, J.H., Vite, C., Yanjanin, N.M., et al. (2013). Identification of Niemann-Pick C1 disease biomarkers through sphingolipid profiling. *J. Lipid Res.* 54, 2800–2814.